Scaling Behavior of Anisotropy Relaxation in Deformed Polymers

Christopher N. Lam,[1,†] Wen-Sheng Xu,[1,†] Wei-Ren Chen,[2] Zhe Wang,[2,3] Christopher B. Stanley,[2]
Jan-Michael Y. Carrillo,[1,4] David Uhrig,[1] Weiyu Wang,[1] Kunlun Hong,[1] Yun Liu,[5,6] Lionel Porcar,[7]
Changwoo Do,[2] Gregory S. Smith,[2] Bobby G. Sumpter,[1,4] and Yangyang Wang[1,*]

[1]*Center for Nanophase Materials Sciences, Oak Ridge National Laboratory, Oak Ridge, Tennessee 37831, USA*
[2]*Oak Ridge National Laboratory, Neutron Scattering Division, Oak Ridge, Tennessee 37831, USA*
[3]*Department of Engineering Physics, Tsinghua University, Beijing 100084, China*
[4]*Oak Ridge National Laboratory, Computational Sciences and Engineering Division, Oak Ridge, Tennessee 37831, USA*
[5]*Center for Neutron Research, National Institute of Standards and Technology, Gaithersburg, Maryland 20899, USA*
[6]*Department of Chemical and Biomolecular Engineering, University of Delaware, Newark, Delaware 19716, USA*
[7]*Institut Laue-Langevin, B.P. 156, F-38042 Grenoble CEDEX 9, France*

Drawing an analogy to the paradigm of quasielastic neutron scattering, we present a general approach for quantitatively investigating the spatiotemporal dependence of structural anisotropy relaxation in deformed polymers by using small-angle neutron scattering. Experiments and nonequilibrium molecular dynamics simulations on polymer melts over a wide range of molecular weights reveal that their conformational relaxation at relatively high momentum transfer Q and short time can be described by a simple scaling law, with the relaxation rate proportional to Q. This peculiar scaling behavior, which cannot be derived from the classical Rouse and tube models, is indicative of a surprisingly weak direct influence of entanglement on the microscopic mechanism of single-chain anisotropy relaxation.

The dynamics of polymers is characterized by a remarkably wide range of length scales and timescales. Historically, the development of quasielastic neutron scattering techniques has provided a powerful tool for understanding the microscopic details of polymer motions in the quiescent state, where the spatial and temporal dependence of dynamics is encapsulated in the measured coherent and incoherent dynamic structure factors or corresponding intermediate scattering functions in Fourier space [1–3]. The application of quasielastic neutron scattering to polymers undergoing mechanical deformation and flow has so far been limited by serious theoretical and practical difficulties, despite some technical progress [4,5]. In this context, time-resolved small-angle neutron scattering (SANS), based on either *ex situ* or *in situ* methods, stands out as a different and alternative approach to elucidating the spatiotemporal relation of molecular motions in the nonequilibrium deformed state.

In this Letter, we describe a *quantitative* method for analyzing the structural anisotropy relaxation of polymers, by drawing an analogy to the paradigm of quasielastic neutron scattering. To illustrate our approach, let us consider the case of small-angle neutron scattering from a mixture of two identical polymers, one deuterated and the other protonated, where the scattering intensity $I(\boldsymbol{Q};t)$ is dominated by the single-chain structure factor $S(\boldsymbol{Q};t)$ [6,7],

$$I(\boldsymbol{Q};t) \propto S(\boldsymbol{Q};t) = \frac{1}{N^2}\sum_{m,n}\langle e^{i\boldsymbol{Q}\cdot[\boldsymbol{R}_n(t)-\boldsymbol{R}_m(t)]}\rangle. \quad (1)$$

Here $\boldsymbol{R}_n$ and $\boldsymbol{R}_m$ are the position vectors of the nth and mth segments of a polymer chain of length N, respectively. The notation $f(\ldots;t)$ is used to emphasize the fact that we are measuring the time *evolution* of the quantity $f(\ldots)$, instead of its time *correlation*. For a step-strain experiment in which the sample is deformed instantaneously at time $t = 0$, $S(\boldsymbol{Q};t)$ describes the relaxation of the perturbed polymer structure towards the equilibrium state. The approach we introduce here exploits the so-called spherical harmonic expansion technique [8–14]. In general, the single-chain structure factor can be decomposed by a series of spherical harmonics: $S(\boldsymbol{Q};t) = \sum_{l,m}S_l^m(Q;t)Y_l^m(\theta,\phi)$, where $S_l^m(Q;t)$ is the expansion coefficient corresponding to each real spherical harmonic function $Y_l^m(\theta,\phi)$. For the aforementioned step-strain relaxation experiment, a class of anisotropic structural relaxation functions $\phi_l^m(Q;t)$ can be defined for all the $l > 0$ terms,

$$\phi_l^m(Q;t) \equiv S_l^m(Q;t)/S_l^m(Q;0). \quad (2)$$

These functions bear an apparent resemblance to the classical intermediate scattering functions and encapsulate

the essential spatial and temporal information about the anisotropic single-chain structure.

To demonstrate the usefulness of this new approach, we performed small-angle neutron scattering experiments on a series of uniaxially deformed polymers at the EQ-SANS beam line at the Oak Ridge National Laboratory and the NGB 30m SANS beam line at the National Institute of Standards and Technology. Our experimental system consisted of isotopically labeled polystyrenes (PS) of three different molecular weights, which we shall refer to as PS30K (h-PS: $M_w = 33.5$ kg/mol; d-PS: $M_w = 35.4$ kg/mol; $h/d = 90:10$), PS100K (h-PS: $M_w = 101$ kg/mol; d-PS: $M_w = 115$ kg/mol; $h/d = 90:10$), and PS500K (h-PS: $M_w = 450$ kg/mol; d-PS: $M_w = 510$ kg/mol; $h/d = 5:95$). Their dynamic mechanical spectra are shown in Fig. 1(a). While PS30K has a weight-average molecular weight approximately two times that of the entanglement molecular weight, its linear viscoelastic spectrum is still characteristic of that of an unentangled melt. On the other hand, the two high molecular weight systems exhibit the typical behavior of entangled polymers. The PS samples were uniaxially elongated on an RSA-G2 solid analyzer in their melt state to a stretching ratio $\lambda = 1.8$, allowed to relax for different amounts of time after the step deformation

[Figs. 1(b)–1(d)], and subsequently quenched to the glassy state by pumping cold air into the environmental test chamber. In our experiments, the time required to effectively freeze the large-scale molecular motions was negligibly small ($\lesssim 0.02\tau_R$) compared to the Rouse or reptation relaxation times, ensuring that the evolution of $S(\mathbf{Q})$ could be captured with sufficient temporal accuracy. More details of the sample characteristics and the experimental procedures are provided in the Supplemental Material [15].

The spherical harmonic expansion technique outlined in our previous work [12] allows us to transform the anisotropic two-dimensional SANS spectra during stress relaxation into plots of wave-number-dependent expansion coefficients (Fig. 2). The axial symmetry of the uniaxial deformation eliminates the dependence of $S(\mathbf{Q}; t)$ on ϕ and forbids all the $m \neq 0$ and odd l terms, namely,

$$S(\mathbf{Q}; t) = \sum_{l:\text{even}} S_l^0(Q; t) Y_l^0(\theta). \qquad (3)$$

In this Letter, we confine ourselves to the analysis of the leading anisotropic expansion coefficient $S_2^0(Q; t)$ and its corresponding relaxation function $\phi_2^0(Q; t) \equiv S_2^0(Q; t)/S_2^0(Q; 0)$. In the Supplemental Material [21], we show that
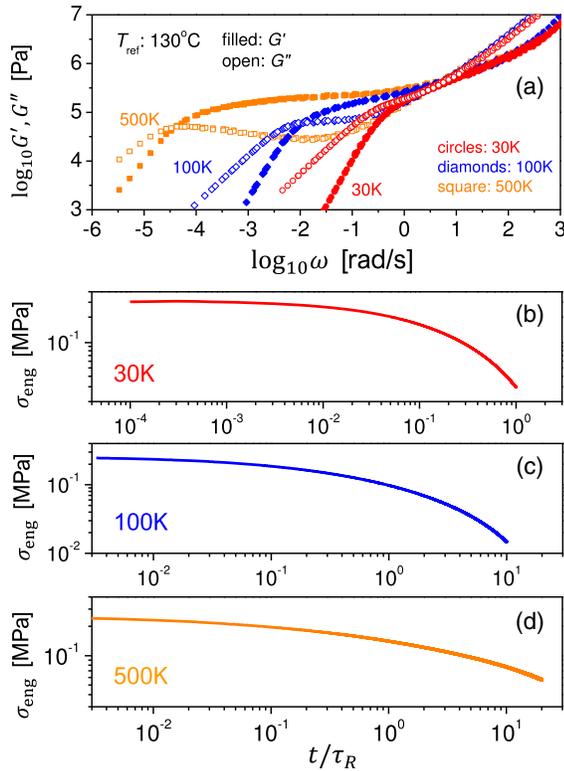

FIG. 1. (a) Dynamic mechanical spectra of PS500K, PS100K, and PS30K at 130 °C. (b)–(d): Relaxation of engineering stress σ_{eng} after a large step uniaxial extension to a stretching ratio $\lambda = 1.8$. The initial Rouse Weissenberg numbers $\text{Wi}_{R,i} = v\tau_R/l_0$ of the step deformation are 5.6, 5.0, and 40, for PS30K, PS100K, and PS500K, respectively.
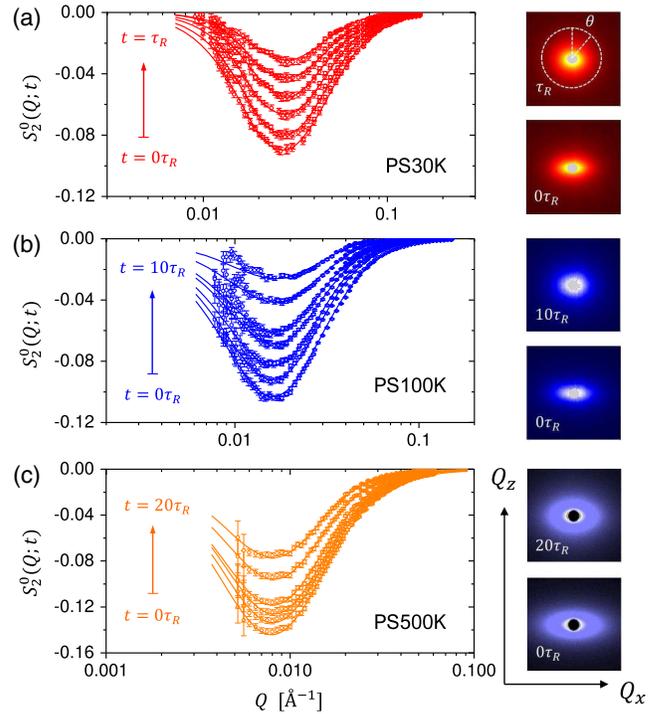
FIG. 2. Relaxation of the leading anisotropic expansion coefficient $S_2^0(Q)$ after a step deformation. (a) PS30K at 0, 0.1, 0.2, 0.4, 0.6, and $1\tau_R$. (b) PS100K at 0, 0.5, 1, 2, 3, 6, and $10\tau_R$. (c) PS500K at 0, 0.5, 1, 3, 10, and $20\tau_R$. (Solid lines) Guide to eye. The SANS spectra at the beginning and the end of the relaxation experiments are shown on the right, with different color schemes for each sample.

according to the classical theory the tensile stress of Gaussian chains is determined by the two-point spatial correlations associated with only the real spherical harmonic function $Y_2^0(\theta, \phi)$. Therefore, $\phi_2^0(Q; t)$ contains the relevant information of the structural changes underlying the macroscopic stress relaxation.

The anisotropic structural relaxation function $\phi_2^0(Q; t)$ can be examined by presenting $\phi_2^0(Q; t)$ as a function of the duration of stress relaxation t at different scattering wave numbers Q [Figs. 3(a)–3(c)]. This approach, in its apparent form, is analogous to the classical way in which the intermediate functions of polymers are analyzed [3]. Here, we focus on the intermediate- and high-Q regions, i.e., $R_g Q \gtrsim 1$, corresponding to length scales that are roughly equal to or smaller than the size of the polymer coil. Figures 3(a)–3(c) reveal that the anisotropy relaxation depends highly on the length scale probed by the scattering experiment—the ϕ_2^0 at high Q's relax much faster than those at low Q's. This result is in accordance with our current general understanding of polymer dynamics. For example, the local segmental relaxation involving a few successive repeating units is much more rapid than the reorientation of the end-to-end vector of the entire polymer chain. However, it is worth noting that neither the affine deformation model [23–25], which assumes the same degree of microscopic deformation on all length scales, nor the speculative formula proposed by de Gennes and Léger [26,27] anticipates such wave number dependence for the anisotropic structural relaxation. For example, the phenomenological approach by de Gennes and Léger predicts that the rate of anisotropy relaxation is independent of Q [26]. To lend support to our experimental observation,

we carried out complementary nonequilibrium molecular dynamics (MD) simulations of the step-strain experiments based on the coarse-grained bead-spring model for polymer melts [28,29]. All beads interact with the Weeks-Chandler-Andersen potential and the bonded interactions between neighboring beads along the polymer chain are described by the finite extensible nonlinear elastic potential. Three different chain lengths, $N = 120$, 500, and 2000, were simulated at $\rho = 0.85$ and $T = 1$ to mirror the PS30K, PS100K, and PS500K samples, respectively. To simulate the step-strain relaxation experiment, the equilibrated polymer melt is uniaxially elongated in the z direction with a constant engineering strain rate to a stretching ratio of $\lambda = 1.8$ and the equilibrium pressure of the melt is imposed in the x and y directions via a Nosé-Hoover barostat. After the step deformation, MD simulations with a Langevin thermostat are performed to study the relaxation behavior. The details of the simulations are described in the Supplemental Material [30]. Figures 3(d)–3(f) show that the MD simulations produce qualitatively similar behavior for the anisotropic structural relaxation function $\phi_2^0(Q; t)$, which further confirms the experimental results.

It is intriguing to ask whether the classical Rouse [40] and tube models [41–43] can offer some insights into the observed spatiotemporal dependence of anisotropy relaxation. Before embarking on the theoretical analysis, we point out a striking feature of the relaxation behavior of $\phi_2^0(Q; t)$, observed in both the SANS experiments and MD simulations. In the case of quasielastic neutron scattering, the so-called Rouse scaling approach, which stems from de Gennes' derivation of the dynamic structure (form) factors of the Rouse model [1,3,44], has been fruitful in elucidating
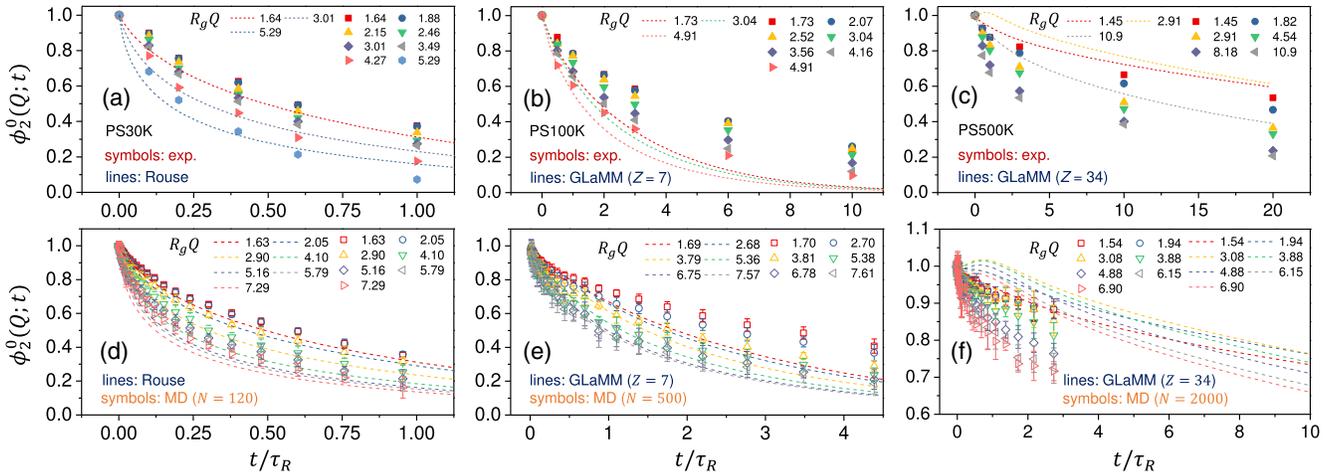

FIG. 3. Anisotropic structural relaxation function $\phi_2^0(Q; t)$ as a function of the normalized relaxation time t/τ_R (with τ_R being the Rouse relaxation time) at different Q's. (a)–(c) Comparison of experiments and theories. (d)–(f) Comparison of simulations and theories. To put these results in perspective, the momentum transfer Q is normalized by the equilibrium radius of gyration R_g of the polymer. The initial Rouse Weissenberg numbers in the MD simulations are 5.56, 6.08, and 41.8 for $N = 120$, $N = 500$, and $N = 2000$, respectively. The same rates are used in the corresponding theoretical calculations. The GLaMM calculations include the "local fluctuation" effect [39].

the slow dynamics of polymer melts. In particular, it has been shown that, for $R_gQ > 1$ and $t < \tau_R$, the coherent intermediate scattering function $F_{\mathrm{coh}}(Q, t)$ can be described as a function of the scaling variable $(\Gamma t)^{1/2}$, where the decay rate $\Gamma \propto Q^4$. Therefore, $F_{\mathrm{coh}}(Q, t)$ measured at different Q and t can be collapsed by plotting $F_{\mathrm{coh}}(Q, t)$ against the Rouse variable $(\Gamma t)^{1/2}$ [44]. Interestingly, we find that the anisotropic structural relaxation functions $\phi_2^0(Q; t)$ at different Q's can be reduced to a single curve by using $(R_gQ)^{1/2}(t/\tau_R)^{1/2}$ as the scaling variable [Fig. 4(a)]. In other words, Fig. 4(a) indicates that $\phi_2^0(Q; t)$ can be cast into the following functional form,

$$\frac{S_2^0(Q; t)}{S_2^0(Q; 0)} = \phi_2^0(Q; t) \sim \exp\left[-(\Gamma t)^{1/2}\right], \qquad (4)$$

with $\Gamma \propto Q$. Furthermore, it appears that the data from the three systems can be further superimposed onto a master curve by normalizing the time t with the longest viscoelastic relaxation time τ [inset of Fig. 4(a)]. Similar to the case of quasielastic neutron scattering, the above scaling approach is only valid under roughly the condition of $R_gQ > 1$ and $t < \tau$. Lastly, the experimentally observed scaling behavior is corroborated by the nonequilibrium MD simulations [Figs. 4(b)–4(d)].

To put these results in perspective, we evaluate the anisotropic structural relaxation function $\phi_2^0(Q; t)$ using the Rouse model for the unentangled system and the tube model by Graham et al. [43], i.e., the GLaMM model, for the entangled polymers [45]. The GLaMM model is solved with the standard parameters in the literature [43]. The comparisons between the theories and simulations are presented in Figs. 3(d)–(f) and 4(b)–4(d). At first glance, the Rouse model seems to be able to provide a reasonable description of the spatiotemporal dependence of anisotropy relaxation for short chains [Figs. 3(a) and 3(d)]. However, a closer inspection reveals that the model does not faithfully reproduce the aforementioned scaling for $\phi_2^0(Q; t)$ [Fig. 4(b)]. Additionally, it should be noted that, for the entangled chains, the scaling behavior persists well beyond the Rouse relaxation time. The observed scaling behavior for anisotropy relaxation, therefore, does not arise from the unconstrained Rouse motion. It is worth mentioning that deviation from the standard Rouse behavior has been observed in neutron spin-echo experiments on an unentangled polyethylene melt in the equilibrium state [44,55] and is attributed to non-Gaussian dynamics. The possible connection between these phenomena remains to be explored.

Figures 3(b), 3(c), 3(e), 3(f), 4(c), and 4(d) indicate that the tube model also fails to predict the correct spatiotemporal dependence for anisotropy relaxation, even with the consideration of local fluctuations about the primitive path [39,45]. We previously showed that the chain retraction
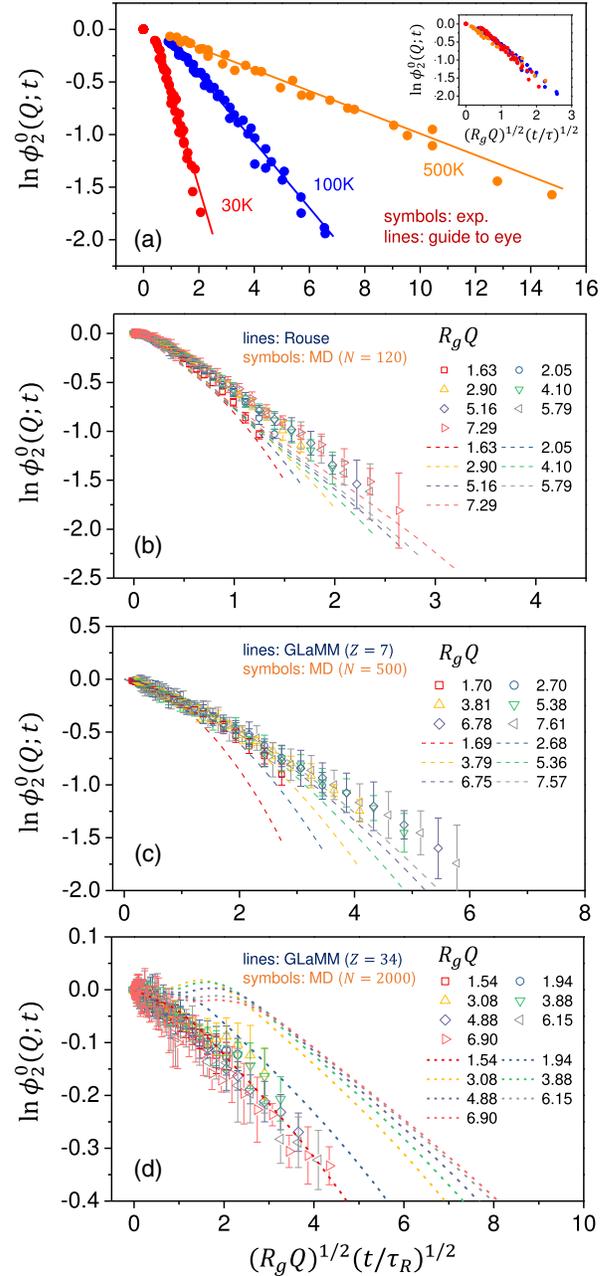

FIG. 4. $\ln[\phi_2^0(Q; t)]$ as a function of the scaling variable $(R_gQ)^{1/2}(t/\tau_R)^{1/2}$. (a) Scaling analysis for the experimental data. (Inset) Shows $\ln[\phi_2^0(Q; t)]$ as a function of $(R_gQ)^{1/2}(t/\tau)^{1/2}$, where τ is the longest viscoelastic relaxation time of the sample. (b)–(d) Scaling analysis of the theoretical and simulation results.

mechanism of the tube model leads to an increase of $S_2^0(Q; t)$ around the Rouse time in the intermediate-Q range after a large step uniaxial deformation, which is inconsistent with both the SANS experiment [12] and the MD simulation [29]. Not surprisingly, quantitative analysis of $\phi_2^0(Q; t)$ reveals a strong deviation from the theoretical prediction for the well-entangled systems (PS500K and the $N = 2000$ chain in simulation). The upturn of the

theoretical $\phi_2^0(Q;t)$ at intermediate Q and $t < \tau_R$ is caused by the chain retraction mechanism [12]. The effect of chain retraction is less pronounced for mildly entangled polymers [29]. Nevertheless, the theory disagrees with both the experiment [Fig. 4(a)] and the simulation [Fig. 4(c)].

The most surprising aspect of our result is that entanglement appears to have a very weak direct influence on the microscopic mechanism of single-chain anisotropy relaxation: the same peculiar behavior is observed for both entangled and unentangled systems. Furthermore, for the well-entangled systems, the scaling law holds well both below ($aQ > 1$) and above ($aQ < 1$) the length scale of the tube diameter a. The effect of entanglement shows up only indirectly through the scaling variable τ [inset of Fig. 4(a)]. This observation suggests a possible simple explanation for the absence of "chain retraction" in the previous step-strain relaxation experiments [12] and molecular dynamics simulations [29]: if the confinement effect of the tube on the test chain is weak, then the molecular relaxation on the timescale of the Rouse time will not produce the unique conformation predicted by the chain retraction mechanism of the tube model [42].

In summary, we present the first quantitative analysis of the spatial and temporal dependence of anisotropy relaxation in deformed polymers by using small-angle neutron scattering and nonequilibrium molecular dynamics simulations. We show that the relaxation of the anisotropic structure of uniaxially stretched entangled and unentangled polymer melts can be described by a simple, universal scaling law, with the relaxation rate proportional to the magnitude of the momentum transfer. This unexpected finding presents a challenge to our current theoretical understanding of the rheological behavior of polymers: the observed scaling behavior of anisotropy relaxation cannot be explained by the classical Rouse and tube models. This Letter highlights the importance of studying the spatiotemporal dependence of molecular motion under deformation and flow—an aspect that has been overlooked in traditional polymer rheology.

*wangy@ornl.gov
†C. N. L. and W.-S. X. contributed equally to this work.

[1] P. G. de Gennes, Physics **3**, 37 (1967).
[2] E. Dubois-Violette and P. G. de Gennes, Physics **3**, 181 (1967).
[3] B. Ewen and D. Richter, Adv. Polym. Sci. **134**, 1 (1997).
[4] W. Pyckhout-Hintzen, S. Westermann, A. Wischnewski, M. Monkenbusch, D. Richter, E. Straube, B. Farago, and P. Lindner, Phys. Rev. Lett. **110**, 196002 (2013).
[5] M. Kawecki, P. Gutfreund, F. Adlmann, E. Lindholm, S. Longeville, A. Lapp, and M. Wolff, J. Phys. Conf. Ser. **746**, 012014 (2016).
[6] P. G. de Gennes, *Scaling Concepts in Polymer Physics* (Cornell University Press, New York, 1979).
[7] J. S. Higgins and H. Benoît, *Polymers and Neutron Scattering* (Clarendon Press, Oxford, 1994).
[8] N. A. Clark and B. J. Ackerson, Phys. Rev. Lett. **44**, 1005 (1980).
[9] D. J. Evans, H. J. M. Hanley, and S. Hess, Phys. Today **37**, No. 1, 26 (1984).
[10] Y. Suzuki, J. Haimovich, and T. Egami, Phys. Rev. B **35**, 2162 (1987).
[11] N. J. Wagner and B. J. Ackerson, J. Chem. Phys. **97**, 1473 (1992).
[12] Z. Wang, C. N. Lam, W.-R. Chen, W. Wang, J. Liu, Y. Liu, L. Porcar, C. B. Stanley, Z. Zhao, K. Hong, and Y. Wang, Phys. Rev. X **7**, 031003 (2017).
[13] G.-R. Huang, Y. Wang, B. Wu, Z. Wang, C. Do, G. S. Smith, W. Bras, L. Porcar, P. Falus, and W.-R. Chen, Phys. Rev. E **96**, 022612 (2017).
[14] G.-R. Huang, B. Wu, Y. Wang, and W.-R. Chen, Phys. Rev. E **97**, 012605 (2018).
[15] See Supplemental Material at http://link.aps.org/supplemental/10.1103/PhysRevLett.121.117801 for details of the sample characteristics and the experimental procedures, which includes Refs. [16–20].
[16] J. D. Ferry, *Viscoelastic Properties of Polymers*, 3 ed. (Wiley, New York, 1980).
[17] K. Osaki, K. Nishizawa, and M. Kurata, Macromolecules **15**, 1068 (1982).
[18] K. Osaki, T. Uematsu, and Y. Yamashita, J. Polym. Sci. Part B: Polym. Phys. **39**, 1704 (2001).
[19] A. E. Likhtman and T. C. B. McLeish, Macromolecules **35**, 6332 (2002).
[20] H. Watanabe, Prog. Polym. Sci. **24**, 1253 (1999).
[21] See Supplemental Material at http://link.aps.org/supplemental/10.1103/PhysRevLett.121.117801 for a brief discussion of the significance of the second expansion coefficient, which includes Ref. [22].
[22] R. G. Larson, *Constitutive Equations for Polymer Melts and Solutions* (Butterworth-Heinemann, London, 2013).
[23] R. Ullman, J. Chem. Phys. **71**, 436 (1979).

[24] R. Muller, C. Picot, Y. Zang, and D. Froelich, Macro-molecules **23,** 2577 (1990).

[25] O. Hassager, K. Mortensen, A. Bach, K. Almdal, H. K. Rasmussen, and W. Pyckhout-Hintzen, Rheol. Acta **51,** 385 (2012).

[26] See Supplemental Material at http://link.aps.org/supplemental/10.1103/PhysRevLett.121.117801 for a brief discussion of the model of de Gennes and Léger.

[27] P. G. de Gennes and L. Léger, Annu. Rev. Phys. Chem. **33,** 49 (1982).

[28] K. Kremer and G. S. Grest, J. Chem. Phys. **92,** 5057 (1990).

[29] W.-S. Xu, J.-M. Y. Carrillo, C. N. Lam, B. G. Sumpter, and Y. Wang, ACS Macro Lett. **7,** 190 (2018).

[30] See Supplemental Material at http://link.aps.org/supplemental/10.1103/PhysRevLett.121.117801 for details of the MD simulations, which includes Refs. [31–38].

[31] W. M. Brown, P. Wang, S. J. Plimpton, and A. N. Tharrington, Comput. Phys. Commun. **182,** 898 (2011).

[32] S. Plimpton, J. Comput. Phys. **117,** 1 (1995).

[33] LAMMPS web page: http://lammps.sandia.gov. The present Letter utilized the version released on March 31, 2017.

[34] J. Cao and A. E. Likhtman, ACS Macro Lett. **4,** 1376 (2015).

[35] R. S. Hoy, K. Foteinopoulou, and M. Kröger, Phys. Rev. E **80,** 031803 (2009).

[36] D. Hossain, M. Tschopp, D. Ward, J. Bouvard, P. Wang, and M. Horstemeyer, Polymer **51,** 6071 (2010).

[37] S. Jabbari-Farouji, J. Rottler, O. Lame, A. Makke, M. Perez, and J.-L. Barrat, ACS Macro Lett. **4,** 147 (2015).

[38] A. J. Parker and J. Rottler, Macromolecules **48,** 8253 (2015).

[39] A. Blanchard, R. S. Graham, M. Heinrich, W. Pyckhout-Hintzen, D. Richter, A. E. Likhtman, T. C. B. McLeish, D. J. Read, E. Straube, and J. Kohlbrecher, Phys. Rev. Lett. **95,** 166001 (2005).

[40] P. E. Rouse, J. Chem. Phys. **21,** 1272 (1953).

[41] P. G. de Gennes, J. Chem. Phys. **55,** 572 (1971).

[42] M. Doi and S. F. Edwards, *The Theory of Polymer Dynamics* (Oxford University Press, Oxford, 1986).

[43] R. G. Graham, A. E. Likhtman, T. C. B. McLeish, and S. T. Milner, J. Rheol. **47,** 1171 (2003).

[44] D. Richter, B. Ewen, B. Farago, and T. Wagner, Phys. Rev. Lett. **62,** 2140 (1989).

[45] See Supplemental Material at http://link.aps.org/supplemental/10.1103/PhysRevLett.121.117801 for discussions of the Rouse and tube models, which includes Refs. [46–54].

[46] A. Onuki, J. Phys. Soc. Jpn. **54,** 3656 (1985).

[47] A. Peterlin, J. Polym. Sci. **23,** 189 (1957).

[48] A. Peterlin, J. Chem. Phys. **39,** 224 (1963).

[49] A. Peterlin, Pure Appl. Chem. **12,** 563 (1966).

[50] A. Peterlin, W. Heller, and M. Nakagaki, J. Chem. Phys. **28,** 470 (1958).

[51] A. Peterlin and C. Reinhold, J. Chem. Phys. **40,** 1029 (1964).

[52] Y. Rabin, J. Chem. Phys. **88,** 4014 (1988).

[53] S. Q. Wang, J. Chem. Phys. **92,** 7618 (1990).

[54] H. Watanabe and T. Inoue, J. Phys. Condens. Matter **17,** R607 (2005).

[55] W. Paul, G. D. Smith, D. Y. Yoon, B. Farago, S. Rathgeber, A. Zirkel, L. Willner, and D. Richter, Phys. Rev. Lett. **80,** 2346 (1998).